Journal of Molecular Spectroscopy **212,** 53–56 (2002)
doi:10.1006/jmsp.2002.8514, available online at http://www.idealibrary.com on IDEAL®

High-Resolution Fourier Transform Study of MgCl: The $A^2\Pi$–$X^2\Sigma^+$ Band System

T. Hirao,* P. F. Bernath,* C. E. Fellows,† R. F. Gutterres,† and M. Vervloet‡

*Department of Chemistry, University of Waterloo, Waterloo, Ontario, Canada N2L 3G1; †Laboratório de Espectroscopia e Laser, Instituto de Física, Universidade Federal Fluminense, Campus da Boa Viagem, Niterói, Rio de Janeiro 24210-340, Brazil; and ‡Laboratoire de Photophysique Moléculaire, Bât. 350, Campus d'Orsay 91405, Orsay Cedex, France

Received August 14, 2001; in revised form December 13, 2001

The $A^2\Pi$–$X^2\Sigma^+$ emission band system of the MgCl molecule has been studied by means of high-resolution Fourier transform spectroscopy. Excited MgCl molecules were produced by two different techniques: (i) at Orsay, they were created by mixing Mg vapor with a flow of He/Cl_2 and excited in a "heated" Schüller-type discharge tube, and (ii) at Waterloo, they were generated by using a copper hollow cathode lamp loaded with $MgCl_2$ powder. Rovibronic analysis of the (0, 0) and (0, 1) bands was performed. Molecular constants were derived in a weighted nonlinear least squares fit, including both the new line positions and the previously published microwave frequencies (M. Bogey, C. Demuynck, and J. L. Destombes, *Chem. Phys. Lett.* **155,** 265 (1989); Y. Ohshima and Y. Endo, *Chem. Phys. Lett.* **213,** 95 (1993)).

I. INTRODUCTION

Alkaline-earth monohalides MX (where M is the metal and X the halogen) have attracted the interest of theoretical and experimental spectroscopists for a long time. These molecules are ionic compounds and have nine valence electrons outside closed atomic shells. The electronic structure of the ground state and the first excited states can be described as an unpaired electron around a molecular ion core consisting of two closed-shell ions, M^{2+} and X^-. Several ionic bonding models have been developed to represent the electronic structure of the low-lying states (*1–3*).

Experimental spectroscopic studies of the MgCl molecule (*4*) have provided information on two band systems, viz., $A^2\Pi$–$X^2\Sigma^+$ and $B^2\Sigma^+$–$A^2\Pi$. The first detailed vibrational analysis of the $A^2\Pi$–$X^2\Sigma^+$ band system was performed by Morgan (*5*). The $B^2\Sigma^+$–$A^2\Pi$ band system was first reported by Rao and Rao (*6*), and a study of the isotope-shifts in this band system was conducted by Darji *et al*. (*7*). The rotational structure of the (0, 0) and (0, 1) bands of the $A^2\Pi$–$X^2\Sigma^+$ system was first studied by Morgan and Barrow (*8*), who assumed that the $A^2\Pi$ state was inverted. Later, Patel and Patel (*9*) analyzed the same bands and determined a set of molecular constants different from those obtained by Morgan and Barrow (*8*). The $A^2\Pi$–$X^2\Sigma^+$ band system was also photographed by Singh *et al*. (*10*), who performed a rotational analysis of the (0, 0), (0, 1), and (0, 2) bands. In their work the spin-doubling splitting of the ground state was resolved for the (0, 1) and (0, 2) bands, and the $A^2\Pi$ state was determined to be regular. Nevertheless, the limited resolution did not permit the direct observation of the spin-doubling splitting in the (0, 0) band, or assignments for the isotopic molecule $^{24}Mg^{37}Cl$. The $B^2\Sigma^+$–$A^2\Pi$ (0, 0) band was photographed and analyzed by Singh *et al*. (*11*), who observed rotational perturbations in the F_2 levels of the $v = 0$ $B^2\Sigma^+$ state. A low resolution vibrational analysis of the $A^2\Pi$–$X^2\Sigma^+$ transition was carried out by Uttam *et al*. in 1992 (*12*).

A millimeter-wave rotational spectrum between 130–290 GHz in the ground state was obtained for the first three vibrational levels by M. Bogey *et al*. (*13*). They performed a global analysis (including all observed vibrational levels) of their data set. Ohshima and Endo (*14*) have studied the rotational spectrum of the $^{24}Mg^{35}Cl$ molecule for $v = 0$ and $v = 1$ by using a Fourier transform microwave spectrometer combined with a laser ablation source. Later, new millimeter-wave measurements, in the region between 260–380 GHz, were carried out by Anderson and Ziurys (*15*). In their work, the hyperfine structure of MgCl was studied and several rotational transitions for $v = 0$ in the ground state of the $^{25}Mg^{35}Cl$, $^{25}Mg^{37}Cl$, $^{26}Mg^{35}Cl$, and $^{26}Mg^{37}Cl$ isotopic species were observed. The $Mg(^1S) + Cl_2$ reaction was studied by Bourguignon *et al*. (*16*) by using laser-induced fluorescence (LIF) detection. They were able to derive a set of molecular constants for the $X^2\Sigma^+$ ($v = 0$ and 1) and $A^2\Pi$ ($v = 0$) states. The $A^2\Pi$ electronic state of the MgCl molecule presents a very interesting feature due to the mixing of a repulsive inverted $^2\Pi_i$ state with the regular $A^2\Pi$ state. As a consequence, the $A^2\Pi$ state undergoes predissociation, which was seen in the laser excitation experiments carried out by Rostas *et al*. (*17*). They observed a cut-off in intensity at $v_A = 7$. By adding the rotationally-resolved data taken from optical (*8, 10*) and millimeter-wave spectra (*13*), these authors performed an

Supplementary data for this article are available on IDEAL (http://www.idealibrary.com) and as part of the Ohio State University Molecular Spectroscopy Archives (http://msa.lib.ohio-state.edu/jmsa_hp.htm).

0022-2852/02 $35.00

analysis of several bands of the A–X electronic transition. The value obtained for the lambda doubling constant, p, was positive, in contrast to the simple theoretical predictions based on the pure precession model (*18*).

We present here a study of the emission spectra of the MgCl $A^2\Pi$–$X^2\Sigma^+$ band system which was recorded using a Fourier transform spectrometer (FTS). Two spectra were recorded independently at Orsay and Waterloo by using different techniques. The strong similarity of the spectra has led to a joint analysis of the data. A complete rovibronic treatment of the $A^2\Pi$–$X^2\Sigma^+$ (0, 0) and (0, 1) bands, including the vibrational dependence of the ground state constants and of the spin–orbit splitting of the $A^2\Pi$ state, was carried out.

II. EXPERIMENT DETAILS

II.1. Orsay Experiment

Excited MgCl molecules were produced in a Schüller-type discharge tube which was heated in the middle. More details on the Schüller discharge device can be found elsewhere (*19*). Briefly, this discharge tube consists of a quartz tube in which both electrodes are protected by liquid nitrogen traps. In this way, contamination of the electrodes is prevented, resulting in a very stable discharge. This light source is particularly convenient for Fourier transform emission spectroscopy. The MgCl molecules were produced in the following way: Mg pellets were introduced into the middle part of the discharge tube, which was heated up to 800°C, in order to obtain Mg vapor. A DC discharge (3 400 V, 100 mA) was established through a flowing He/Cl_2 gas mixture (1% Cl_2 in He) at a pressure of 22.5 Torr. The spectrum was recorded by means of a Bruker IFS 120 HR Fourier transform spectrometer. The detector was a photomultiplier tube (HAMAMATSU 1P28) associated with a long-pass colored glass filter. The spectrum was obtained after the transformation of 1 000 co-added interferograms recorded at an apodized resolution of 0.060 cm^{-1}. Wavenumbers and intensities of the lines were determined with the standard Bruker OPUS software.

II.2. Waterloo Experiment

In Waterloo, the emission spectra of MgCl were generated by using a copper hollow cathode lamp. A few grams of the $MgCl_2$ salt (Aldrich, 99%) were placed in a hollow cathode that was 5 cm long and 1 cm inner diameter. The cathode was inside a water-cooled stainless steel chamber. A flow of 5 Torr of helium buffer gas was maintained through the chamber, and a current of 330 mA DC was used. The DC discharge vaporized the sample and made a bright emission inside the hollow cathode. The emission was focused with a CaF_2 lens into the entrance aperture of the spectrometer. The spectra were recorded with Bruker IFS 120 HR Fourier transform spectrometer, modified to record double-sided interferograms (*20, 21*). The photomultiplier tube was attached to the "back parallel exit" of the spectrometer to improve sensitivity. In the measurement, the discharge generated several intense atomic transitions of magnesium, which severely degraded the signal-to-noise ratio. Because of this, we inserted a 450-nm blue pass filter (CORION, LS-450) just in front of the photomultiplier tube to cut the intense atomic lines present near 19 000 cm^{-1} (*22*). A visible quartz beamsplitter was used for the measurement. The spectral region covered was from 19 000 to 28 000 cm^{-1} at a resolution of 0.03 cm^{-1}. The spectra were collected in a 1.5-h accumulation of scans. The spectral line positions were measured by using the PC-DECOMP program developed by J. Brault. During this measurement, several electronic transitions of the CuCl by-product were identified around 23 000 cm^{-1} (*21*). All line positions were calibrated with the standard atomic lines of helium. The helium atomic line positions were obtained in a separate measurement of the emission spectrum from a DC discharge of a mixture of helium and argon, calibrated using the known argon atomic lines (*23*). The calibration factor was 1.000001672 for our MgCl spectrum. Observed line positions are provided in the journal electronic data archive.

III. RESULTS

The observed high line density (Fig. 1) caused by overlapping branches of this emission spectrum is a consequence of both the doublet structure in the electronic states and the very similar potential curves of the upper and lower states. In a $A^2\Pi$–$X^2\Sigma^+$ electronic transition one can expect to observe 12 branches for each band (*24*). In addition, these electronic states have similar vibrational (and rotational) constants, resulting vibrational sequences in which the separations of the bands are about 30 cm^{-1}.

An overview of a part of the obtained spectrum is shown in Fig. 1. The $A^2\Pi$–$X^2\Sigma^+$ (0, 0) band can be seen clearly in this figure, which shows the bandheads of the branches, P_{12}, P_{11}, P_{22}, Q_{22}, for the (0, 0) band, as well for the weaker (1, 1) band.

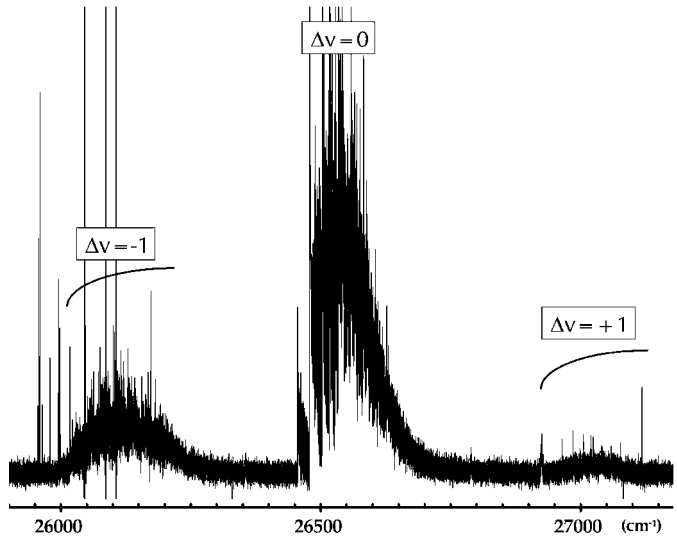

FIG. 1. Overview of the A–X spectrum of MgCl.

Only the lines of the (0, 1) $A^2\Pi_{1/2}$–$X^2\Sigma^+$ subband could be assigned in the $\Delta v = -1$ sequence.

Previously unobserved spin-doubling (*10*) in the $A^2\Pi$–$X^2\Sigma^+$ (0, 0) band system could be directly seen, for example, from the assignment of the splitting of the Q_{12}, R_{22} pair of branches. Rotational structure for the P_{12} branches for both the $^{24}Mg^{35}Cl$ and the $^{24}Mg^{37}Cl$ isotopic species could be easily identified.

IV. ANALYSIS

For the fitting, we utilized the conventional $\mathbf{N^2}$ reduced Hamiltonian (*25*) with Hund's case (a) basis functions for the $A^2\Pi$ state, while the Dunham expansion formula (1) was applied to the ground $X^2\Sigma^+$ state (*26*):

$$E = \sum_{i,j} Y_{ij}\left(v+\frac{1}{2}\right)^i [N(N+1)]^j + \begin{cases} \frac{1}{2}N\sum_{i,j}\gamma_{ij}\left(v+\frac{1}{2}\right)^i [N(N+1)]^{(j-1)} \\ \quad \left(e: J = N+\frac{1}{2}\right) \\ -\frac{1}{2}(N+1)\sum_{i,j}\gamma_{ij}\left(v+\frac{1}{2}\right)^i [N(N+1)]^{(j-1)} \\ \quad \left(f: J = N-\frac{1}{2}\right) \end{cases} \quad [1]$$

To improve the molecular constants, we also included microwave data for the $v = 0, 1, 2$ vibrational levels from Bogey *et al.* (*13*) and Fourier transform microwave data ($v = 0, 1$) from Ohshima and Endo (*14*) after correcting for the effects of hyperfine structure. The accuracy of line positions in the A–X transition is estimated to be better than 0.005 cm^{-1} if all lines were completely resolved. However, almost all lines were overlapped because of the small spin–orbit interaction in the $A^2\Pi_r$ state ($A_{SO} \sim 54$ cm^{-1} for $v' = 0$) and the compact vibrational structure in the $\Delta v = 0$ and 1 sequences. Because of this, we found the accuracy of the A–X transitions for (0, 0) and (0, 1) bands poorer than initially expected. In the (0, 0) band, uncertainties for P_{12}, Q_{11}, and Q_{22} branches were assumed to be 0.005, 0.01, and 0.025 cm^{-1}, respectively, while for the other branches in (0, 0) band and for the F_1 spin component in (0, 1) band the uncertainties were assumed to be 0.05 cm^{-1}. The obtained molecular constants for the $X^2\Sigma^+$ and $A^2\Pi$ states are listed in Table 1 and Table 2, respectively. The molecular constants obtained by Rostas *et al.* (*17*) are listed in the tables for comparison. The obtained molecular constants in both $X^2\Sigma^+$ and $A^2\Pi$ states are generally in excellent agreement with those of Rostas *et al.* (*17*). We were also now able to determine a value for the Λ-doubling constant, q, in the $A^2\Pi$ state. An additional constant, Y_{21}, and improved values for the other constants (Table 1) were determined for the ground state as compared to the fit of Ohshima and Endo (*14*). This was possible because of the inclusion of the previous microwave data (*13, 14*) and the accuracy of our FTS data. Note that our $\Delta G_{\frac{1}{2}}$ value of 462.1013(18) cm^{-1} is in excellent agreement with the value of 462.10 cm^{-1} calculated from $w_e = 466.20$ cm^{-1} and $w_e x_e = 2.05$ cm^{-1} obtained from the band head analysis of Uttam *et al.* (*12*) and with the value of 462.114 cm^{-1} of Rostas *et al.* (*17*).

TABLE 1
MgCl $X^2\Sigma^+$ Constants

Constant	$X^2\Sigma^{+a}$	$X^2\Sigma^{+b}$
Y_{10}	462.1013(18)[c]	466.08
Y_{01}	0.245615499(41)	0.245611
$Y_{02} \times 10^{+7}$	−2.72581(55)	−2.7265
$Y_{11} \times 10^{+3}$	−1.620538(52)	−1.610
$Y_{12} \times 10^{+10}$	3.29(56)	3.4
$Y_{21} \times 10^{+6}$	3.589(16)	—
$\gamma_{01} \times 10^{+2}$	0.223479(29)	0.2227
$\gamma_{11} \times 10^{+5}$	−3.015(25)	−3.0
$\gamma_{02} \times 10^{+9}$	−9.08(50)	—

Note. In column (a), molecular constants in cm^{-1} for the $X^2\Sigma^+$ electronic state determined in the analysis from a nonlinear least-squares fit of the global data set. Column (b) shows, for comparison, the values obtained by Rostas *et al.* (*17*). Numbers in parentheses represent one standard deviation in units of the last figure quoted.

[a] This work.

[b] Rostas *et al.* (*17*).

[c] $\Delta G_{\frac{1}{2}}$ value.

TABLE 2
MgCl $A^2\Pi$ Constants

Constant	$A^2\Pi^a$	$A^2\Pi^b$
T_0[c]	26739.91370(142)	26741.33
B_0	0.25082566(82)	0.2517
$D_0 \times 10^{+7}$	2.66932(144)	2.68
A_0	54.4681(20)	55.2
$p_0 \times 10^{+3}$	3.710(59)	5.41
$q_0 \times 10^{+5}$	−6.883(141)	—

Note. In column (a), molecular constants in cm^{-1} for the $A^2\Pi$ electronic state determined in the analysis from a nonlinear least-squares fit of the global data set. Column (b) shows, for comparison, the values obtained by Rostas *et al.* (*17*). Numbers in parentheses represent one standard deviation in units of the last figure quoted.

[a] This work.

[b] Rostas *et al.* (*17*).

[c] Origin of the energy scale is at $v = -\frac{1}{2}$, $N = 0$ of the ground state (i.e., $T_e = 0$).

V. DISCUSSION

In the $A^2\Pi_r$ state, the Λ-doubling constants, p and q, were determined to be $+3.710\,(59) \times 10^{-3}$ and $-6.881(141) \times 10^{-5}$ cm^{-1}, respectively. The simple pure precession expression resulting from Van Vleck transformation of the $A^2\Pi$ and $B^2\Sigma^+$ energy matrix (*18*) is often used to interpret these parameters,

$$p \approx 2\frac{\langle A^2\Pi_{1/2}|\mathbf{H}_{SO}|B^2\Sigma_{1/2}\rangle\langle^2\Pi_{3/2}|B(r)L_+|B^2\Sigma_{1/2}\rangle}{E_A - E_B}$$
$$\approx 2\frac{A_{SO}Bl(l+1)}{E_A - E_B} \quad [2]$$

and

$$q \approx 2\frac{\langle^2\Pi_{3/2}|B(r)L_+|B^2\Sigma_{1/2}\rangle^2}{E_A - E_B}$$
$$\approx 2\frac{B^2l(l+1)}{E_A - E_B}, \quad [3]$$

in which l is an atomic orbital angular momentum ($l = 1$) and A_{SO} and B are the spin–orbit interaction constant and the rotational constant of the $A^2\Pi_r$ state, respectively. "$E_A - E_B$" is the energy difference between the $A^2\Pi$ and $B^2\Sigma^+$ states, which is about $-21\,150$ cm^{-1} (*11*). These formulae thus give $p = -2.58 \times 10^{-3}$ and $q = -1.19 \times 10^{-5}$ cm^{-1}, in contrast to the experimental values. This indicates that simple pure precession does not work for MgCl. A similar situation was found for MgBr (*20*).

In our previous paper, on MgBr (*20*), we cited Rostas *et al*. (*17*), who attributed anomalous sign of the Λ-doubling constants to an interaction with a repulsive $^2\Pi_i$ state. Field (*27*), however, has pointed out that a better explanation is the spin polarization of the Br^- orbitals by the Mg^+ ion. The unpaired electron on Mg^+ polarizes the $|\alpha\rangle$ and $|\beta\rangle$ electrons on the Br^- orbital to a different extent and leaves a net spin polarization on the nominally closed-shell halide anions. This spin polarization contributes to the spin–orbit coupling in the $A^2\Pi$ state and to the anomalous Λ-doubling. This model explains why the spin–orbit constant of MgBr (110 cm^{-1} (*20*)) is bigger than that of Mg^+ (61.0 cm^{-1} (*28*)), and it allows the Λ-doubling constant, p, of MgBr to be positive (*27*). This phenomenon is also expected in the $A^2\Pi_r$ state of MgI, which has not yet been studied by means of high-resolution spectroscopy. However, the spin–orbit constant of MgCl (54.4 cm^{-1}) is close to that of Mg^+, indicating that the polarization effect is, as expected, smaller for MgCl.

VI. CONCLUSION

The $A^2\Pi$–$X^2\Sigma^+$ band system of the MgCl was studied by Fourier transform spectroscopy. The MgCl molecules were produced by two different techniques. An improved set of molecular constants was derived from a rovibronic analysis of the (0, 0) and (0, 1) bands taking into account the microwave measurements of the three lower vibrational levels of the electronic ground state obtained previously (*13, 14*). The spin-doubling (*11*) in the $A^2\Pi$–$X^2\Sigma^+$ (0, 0) band could be assigned and the $A^2\Pi$ electronic state was found to be regular. An unexpected positive value for the Λ-doubling constant p was found and attributed to a spin polarization effect.

ACKNOWLEDGMENTS

We are grateful to Professor R. W. Field (MIT) for valuable suggestions on the interpretation of the lambda doubling constants. This work is partially supported by CAPES/COFECUB (Brazil/France cooperation) 182/96. The authors thank Dr. Daniel Cossart for the loan of the Schüller discharge tube. One of the authors (C.E.F.) thanks CAPES/Brasil for a postdoctoral grant. Support was also provided by the Natural Sciences and Engineering Research Council of Canada.

REFERENCES

1. T. Törring, W. E. Ernst, and S. Kindt, *J. Chem. Phys.* **90,** 4927–4932 (1989).
2. T. Törring, W. E. Ernst, and J. Kändler, *J. Chem. Phys.* **81,** 4614–4619 (1984).
3. S. F. Rice, H. Martin, and R. W. Field, *J. Chem. Phys.* **82,** 5023–5034 (1985).
4. K. P. Huber and G. Herzberg, *in* "Molecular Spectra and Molecular Structure IV." Constants of Diatomic Molecules, Van Nostrand Reinhold Co., New York, 1979.
5. F. Morgan, *Phys. Rev.* **50,** 603–607 (1936).
6. V. S. N. Rao and P. T. Rao, *Indian J. Phys.* **37,** 640–644 (1963).
7. A. B. Darji, N. R. Shah, P. M. Shah, M. B. Sureshkumar, and G. S. Desai, *Pramana* **25,** 571– (1985).
8. E. Morgan and R. F. Barrow, *Nature (London)* **192,** 1182 (1961).
9. M. M. Patel and P. D. Patel, *Indian J. Phys.* **42,** 254–259 (1968).
10. M. Singh, G. S. Ghodgaokar, and M. D. Saksena, *Can. J. Phys.* **65,** 1594–1603 (1987).
11. M. Singh, M. D. Saksena, and G. S. Ghodgaokar, *Can. J. Phys.* **66,** 570–575 (1988).
12. K. N. Uttam, R. Gopal, and M. M. Joshi, *Indian J. Phys. B* **66,** 379–388 (1992).
13. M. Bogey, C. Demuynck, and J. L. Destombes, *Chem. Phys. Lett.* **155,** 265–268 (1989).
14. Y. Ohshima and Y. Endo, *Chem. Phys. Lett.* **213,** 95–100 (1993).
15. M. A. Anderson and L. M. Ziurys, *Chem. Phys. Lett.* **224,** 381–390 (1994).
16. B. Bourguignon, M.-A. Gargoura, J. Rostas, and G. Taieb, *J. Phys. Chem.* **91,** 2080–2086 (1987).
17. J. Rostas, N. Shafizadeh, G. Taieb, B. Bourguignon, and M. G. Prisant, *Chem. Phys.* **142,** 97–109 (1990).
18. H. Lefebvre-Brion and R. W. Field, *in* "Perturbations in the Spectra of Diatomic Molecules." Academic Press, Orlando, FL, 1986.
19. J. H. Callomon, *Can. J. Phys.* **34,** 1046–1074 (1956).
20. T. Hirao, B. Pinchemel, and P. F. Bernath, *J. Mol. Spectrosc.* **202,** 213–222 (2000).
21. T. Parekunnel, L. C. O'Brien, T. L. Kellerman, T. Hirao, M. Elhanine, and P. F. Bernath, *J. Mol. Spectrosc.* **206,** 27–32 (2001).
22. F. M. Phelps III, *in* "M.I.T. Wavelength Tables. Vol. 2. Wave-lengths by Element." MIT Press, Cambridge, MA, 1982.
23. G. Norlén, *Phys. Scr.* **8,** 249–268 (1973).
24. G. Herzberg, *in* "Molecular Spectra and Molecular Structure. I. Spectra of Diatomic Molecules." Van Nostrand Reinhold, New York, 1950.
25. J. M. Brown, E. A. Colbourn, J. K. G. Watson, and F. D. Wayne, *J. Mol. Spectrosc.* **74,** 294–318 (1979).
26. R. D. Urban, U. Magg, H. Brik, and H. Jones, *J. Chem. Phys.* **92,** 14–21 (1990).
27. R. W. Field, personal communication.
28. C. E. Moore, *in* "Atomic Energy Levels as Derived from the Analysis of Optical Spectra," Vol. I. NSRDS, Washington DC, 1971.